Comparison of Three Innovative Technologies for 3D-Acquisition, Modelling, and Visualization of an Underground Mine

Valens FRANGEZ, Benjamin KRAMIS,
Florian HÜBSCHER, Andreas BAUMANN (Switzerland)

Key words: Terrestrial Laser Scanning, SLAM, Indoor Mobile Mapping, Underground Mine Surveying, Virtual Reality, VR

SUMMARY

Mobile mapping (MM) solutions represent an innovative and effective approach for acquiring geospatial information. While outdoor MM solutions are well established, mapping large-scale indoor or underground environments with high surface complexity, detail and possibly low ambient light is still a demanding task, and a variety of technological solutions start to emerge. In this contribution, we compare three such solutions empirically with respect to data quality, properties of the derived 3D models, and usability.

The analysis is based on data collected in a former gold mine using three different techniques. A FARO Focus3D X330 was used to capture approximately 350 metres of underground galleries employing terrestrial laser scanning. About 120 scans were taken within nine hours to cover the entire space. Additionally, the same space was mapped independently using two commercial MM systems suitable for indoor applications, namely a GeoSLAM ZEB-REVO handheld scanner and a Leica Pegasus:Backpack MM system. Each of them required less than 20 minutes for acquiring the galleries in a single walkthrough. A geodetic terrestrial network was established within the mine. Spherical targets placed in the scene and connected to the network were used as a reference for the evaluation of the quality of the point clouds. A 3D model was generated, fused with a digital terrain model and geological maps, and visualized in a virtual reality environment using the HTC Vive headset.

We present the tools and procedures used for data acquisition, model derivation and visualization including generation of fly-through videos. We also assess the solutions in terms of quality, time consumption, complexity of the data processing, and potential use cases, giving recommendations for tackling similar mapping and modelling tasks for underground or indoor environments. None of the solutions stands out as the single optimum one. Rather, the choice of the most appropriate solution depends on the intended application of the resulting 3d models. Relevant questions are e.g., whether high accuracy, low cost for data acquisition or photorealistic appearance are required. The MM solutions prove especially useful when a local precision of a few cm is required but the absolute accuracy is of minor importance. Ground control points throughout the mine could be used to improve the absolute accuracy. High time consumption for both, scanning and preprocessing of the data (i.e. manual registration, etc.),

was recognized as the major downside of the terrestrial laser scanner as compared to the MM solutions.

Comparison of Three Innovative Technologies for 3D-Acquisition, Modelling, and Visualization of an Underground Mine

Valens FRANGEZ, Benjamin KRAMIS,
Florian HÜBSCHER, Andreas BAUMANN (Switzerland)

1. INTRODUCTION

Mobile mapping (MM) solutions represent an innovative and effective approach for acquiring geospatial information. Mapping large-scale indoor or underground environments with high surface complexity, detail and possibly low ambient light is still a demanding task and a variety of technological solutions start to emerge. Integrated geodetic solutions and systems addressing these challenges are being developed for commercial purposes. The paper shows the advantages and disadvantages of such solutions when scanning underground environments by comparing the results to a standard approach employing a terrestrial laser scanner (TLS). We use a 350 m long section of the former gold mine "La miniera d'oro di Sessa" (Switzerland) as a study case. This is a particularly challenging underground environment because of the small tube diameter (1.5 to 3 m).

The empirical comparison is based on data collected using three different instruments: a FARO Focus3D X330 (F3D) terrestrial laser scanner, a Leica Pegasus:Backpack (LPB) MM system and a GeoSLAM ZEB-REVO (ZEB) handheld MM system. We compare the point clouds obtained using these instruments and the respective post-processing software addressing data quality, properties of the derived 3D models, and usability of the instruments. The accuracy of the point clouds is analysed using a geodetic network. Finally, we report about various approaches to visualization of the point clouds including a virtual reality (VR) environment, a fly-through video animation and publication of interactive 3D models on a website.

Similar topics have also been addressed by other authors in recent publications. They either address challenges of underground scanning or present emerging MM solutions. (Sirmacek et al., 2016) carried out a comparison of a terrestrial laser scanner and a MM system focusing on their performance in the interior of a building. The challenge of mapping long and smooth underground environments using a hand-held scanner is addressed in (Farella, 2016). Furthermore, (Zlot et al., 2014) introduced an approach to underground mapping in the absence of GPS by using a custom-built MM system. The past study cases show that the topic is relevant and interesting for research from both, commercial and scientific point of view.

The paper is organized as follows. Section 2 presents the used methods including the instruments and the acquisition process. Point cloud processing and geometric quality are described in the section 3. Section 4 explains several different visualization approaches and

Section 5 presents the comparison of the results. Section 6 concludes the paper and gives recommendations for future tasks.

2. FIELDWORKD AND PREPROCESSING

2.1 Instruments

The instruments used are shown in Figure 1. They differ in terms of handling, setup, data acquisition process, and instrument specifications. Table 1 summarizes some instrument specifications relevant for the carried-out project.

Figure 1: From left to right: FARO Focus3D X330[1], Leica Pegasus:Backpack[2], GeoSLAM ZEB-REVO[3]

According to the specification, the F3D TLS has the lowest ranging error of the instruments used. It offers the possibility to modify the acquisition settings, namely data resolution and quality, scan range, use of additional sensors during the scanning (e.g. compass, altimeter, GPS or inclinometer) and a possibility to acquire colour information. Scanning with a lower resolution allows faster capture of the environment and vice versa. During the scanning process, the instrument must be mounted on a tripod. The acquired raw data are used to generate single point clouds that are registered using the appropriate software (e.g. FARO Scene software).

The LPB is a wearable MM solution consisting of a backpack and a tablet for remote control of the acquisition. The backpack is equipped with five cameras and two LiDAR profilers. Additionally, data obtained with a GNSS antenna allow instant georeferencing of the acquired data when satellite visibility and GNSS signal data quality are sufficient. An inertial measurement unit (IMU) supports the georeferencing and aids in bridging GNSS data gaps. For colouring the point clouds, spherical images are generated by stitching the images of all five cameras together and projecting the RGB values onto the acquired point cloud. When mapping dark areas an additional lighting device can be attached to the backpack. Additionally, the frame rate of images and the camera exposure time can be modified. The acquired raw data are pre-

[1] www.faro.com/en-gb/news/the-new-faro-laser-scanner-focus3d-x-330-the-perfect-instrument-for-3d-documentation-and-land-surveying-2
[2] https://leica-geosystems.com/products/mobile-sensor-platforms/capture-platforms/leica-pegasus-backpack
[3] https://geoslam.com/technology

processed and used to compute the 3D point clouds. The corresponding software uses a SLAM algorithm combining laser scanning data with the GNSS/IMU data.

The ZEB is a handheld scanner that includes a 2D time-of-flight laser range scanner, which is coupled to an IMU. No settings can be modified before the acquisition process. The operator holds the scanner head while the data logger is carried along in a backpack. The environment within the scanning range is acquired by a slow walking speed. Each scanning session is limited to a maximum of 30 min. The acquired raw data are used to compute a point cloud using the GeoSLAM Desktop software. The software uses a SLAM algorithm for creating a single 3D point cloud.

Table 1: Instrument specifications according to the data sheets

	F3D[4]	LPB[5]	ZEB[6]
Weight (with batteries)	5.2 kg	13.7 kg (backpack)	1.0 kg (scanning head) 4.1 kg (carry case)
Size	24 x 20 x 10 cm³	73 x 27 x 31 cm³	8 x 11.3 x 14 cm³ (scanning head) 47 x 22 x 18 cm³ (carry case)
LiDAR type	Proprietary	2 x Velodyne VLP-16	Hokuyo UTM-30LX
Ranging error	2 mm	20 – 30 mm	10 – 30 mm
Operation range (distance measurement)	0.6 – 330 m	1 m – 100 m[7]	0.1 – 20 m
Acquisition	up to 976'000 pts/sec	600'000 pts/sec	43'200 pts/sec

2.2 Data collection

2.2.1 Geodetic terrestrial network

A geodetic terrestrial network was established within the mine and at its entrance. It serves as a reference for the quality assessment of the acquired point clouds. The network consists of two parts, a portal network (8 points) and a subterraneous tunnel network (14 traverse points and 56 fixed points). The network measurements were carried out using a Leica TS60 total station. The position of each fixed point had been planned such that it is visible from at least two traverse points, the next and the previous one. Selected fixed points realised by bolts (holding prisms during network measurements, and holding spheres later) served as the connection between the network measurements and the acquired point clouds.

[4] https://faro.app.box.com/s/4f908b59hcjjj8mezdr58z6n4qy5neli
[5] https://leica-geosystems.com/-/media/files/leicageosystems/products/datasheets/leica_pegasusbackpack_ds.ashx?la=en
[6] http://download.geoslam.com/docs/zeb-revo/ZEB-REVO%20User%20Guide%20V3.0.0.pdf
[7] V.Marini, Geosoft srl / Leica Geosystems, personal communication (5.3.2018)

A minimum variance adjustment within a local coordinate system was carried out using the portal network points as datum points. The standard deviations (1σ) as adjustment results for the last network point in the mine are 5 mm, 14 mm and 1 mm in X, Y and H direction, respectively.

2.2.2 Point cloud acquisition

The mine has a rough surface producing significant occlusions. Inside the mine, sparsely distributed lamps provide low ambient lighting, leading to difficulties for acquiring surface colour. The scanning workflow is different for the different instruments used, in particular because MM relies on sensor motion during acquisition and requires input for bias/drift mitigation (e.g. loop closures, short stops of the motion, etc.) while TLS needs to be static during the measurement and thus requires careful selection of the instrument set-up locations to obtain sufficient coverage. Some properties of the acquisition are gathered in the Table 2. The spheres (diameters of 12 cm and 15 cm) were installed on selected points of the geodetic network. With the standard TLS approach, they are used for registration. However, they also mark reference points within the mine such that they can be identified and located within the point clouds thus serving as a vital component for dataset comparison and quality analysis. During the acquisition using MM, three spheres were placed at the entrance of the mine and three at the far end of the mapped part of the mine. Ten more spheres were placed at locations in between.

Since the F3D is stationary while scanning, occluded areas need to be identified and scanned from additional stations. We used 117 stations to capture the rough surface in the long narrow space inside the mine. Each scan took about five minutes. Due to the low scanner-to-surface distances and in order to speed up the scanning process the ¼-resolution option (244’000 pts/sec) was selected and no images were taken using the internal camera. These images would likely have been of limited use due to the lighting conditions. Registration was planned to be carried out using targets instead of the point cloud itself; thus, at least three reference spheres had to be covered commonly in any pair of point clouds.

The LPB allows to capture the whole mine in a single walkthrough at walking speed. The acquisition using LPB started outside the mine in order to have the system initialized and the data georeferenced based on the GNSS measurements. Performing the measurement in a closed loop and placing the backpack at the initial position again at the end of the acquisition allows the software to better correct for unavoidable time dependent drift even in absence of GNSS. Having such loop closures or collecting data in double passes is a prerequisite to achieve the accuracies specified in the data sheet. A further means to reduce drift effects is the use of zero-velocity updates enabled by the operator stopping movement for a few seconds every few minutes. While the LPB is a very versatile MM system, the specific mine was at the limit of its applicability because (i) the acquisition process was physically demanding for the operator who

had to stoop constantly in order to avoid hitting the walls or ceiling with parts of the sensor assembly within the narrow and low galleries, and (ii) the acquired surfaces were close to or even below the minimum range of the system.

The acquisition process using the ZEB was done in a loop, ending approximately at the same position as started. The sensor is swung while walking such that the point cloud produced by the 2d-profile scanner covers the entire surfaces to be mapped. The walking speed can be slowed down to increase the effective point density at areas where this is needed. In the present study, this was done near the spheres at fixed points in order to assure that they are densely covered.

Table 2: Key parameters of the acquisition

	F3D	LPB	ZEB
Time [min]	540	10	16
Points [million]	5064	25	27
Raw data size [GB]	17	1	0.1
Radiometric data	Intensity	RGB	/

3. POINT CLOUD PROCESSING AND GEOMETRIC QUALITY

3.1 Single-system processing

It is necessary to carry out a single-system processing (registration, data cleaning, subsampling, etc.) on the point clouds before the acquired data are ready for comparison. The available F3D is not able to register directly in the field; we chose to register the F3D scans using the spheres and FARO Scene. The registration is calculated automatically once the centres of the spheres are available, however identifying them required manually clicking on all the spheres, which appear in the individual scans (in total approximately 600 clicks). The registered data can be subsampled and exported into a common data format as single point clouds or complete point cloud. We used the open source software CloudCompare for manual removal of the clutter, which in this project resulted from mirroring effects in the puddles on the floor and other unintentional features.

Leica carried out the collection and pre-processing of the LPB data. Georeferenced point clouds with RGB colour, down-sampled to a nearly homogeneous point density of about 1/2.5 cm using a voxel-based filter were provided for the present analysis. There are indications that the glass of one scanner of the backpack may have been scratched. Additionally, due to the very limited space inside the mine, the loop closure was not possible and the initialization before entering the mine was impaired by poor GNSS availability. Therefore, the available dataset represents only a one-way direction of acquisition and its accuracy and noise level do not correspond to the potential of this MM system as specified in the data sheet. Unwanted features

(e.g. people, top part of the GNSS antenna) have been removed manually from the point cloud for the further analysis.

The ZEB raw data were pre-processed using the corresponding software GeoSLAM Desktop and exported in the selected data format. The fully automatic computing of the point cloud took about 90 min on standard Windows PC, i.e. six times the time needed for data acquisition (16 min). There was hardly any need for subsequent manual cleaning.

3.2 Initial quality analysis

Irrespective of any potential prior georeferencing we decided to transform all point clouds into a common local coordinate system for further processing. This coordinate system is defined by the centres of two spheres (baseline of 20 m) within the mine, but close to its entrance (Figure 2). One point is fixing the position and the other one the rotation around z-axis. There are no rotations around other axis applied, as the point clouds include the respective instrument's determination of the horizontal plane. By comparing the coordinates of the remaining estimated sphere centres to the network coordinates the lateral, longitudinal (scale) and height displacements are determined. As there is only one dataset acquired for each instrument, no statement about repeatability is possible, and the results just represent indicative snapshots. The calculated displacements visualised in Figure 3 reveal that the lateral deviations obtained after georeferencing to the local coordinate system using only the two points near the entry of the mine reach metre-level at the far end (inside the mine). Height and longitudinal displacements are much lower while still showing significant drift. The results obtained using the LTS (F3D) are significantly better as compared to the ground truth than the SLAM-based techniques.

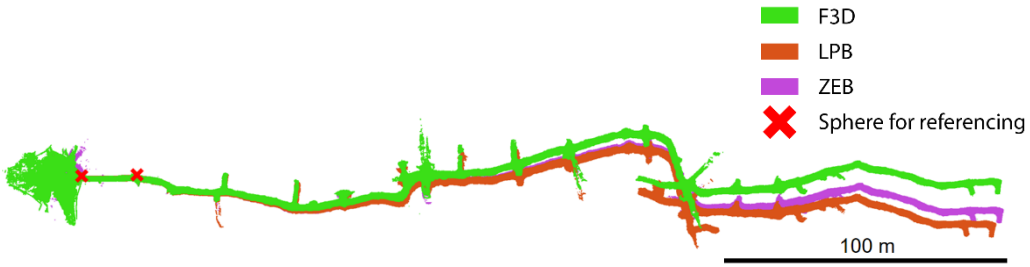

Figure 2: Aligned point clouds, using a 20-metre baseline, show significant discrepancies of a multiple of the mine's diameter (top view)

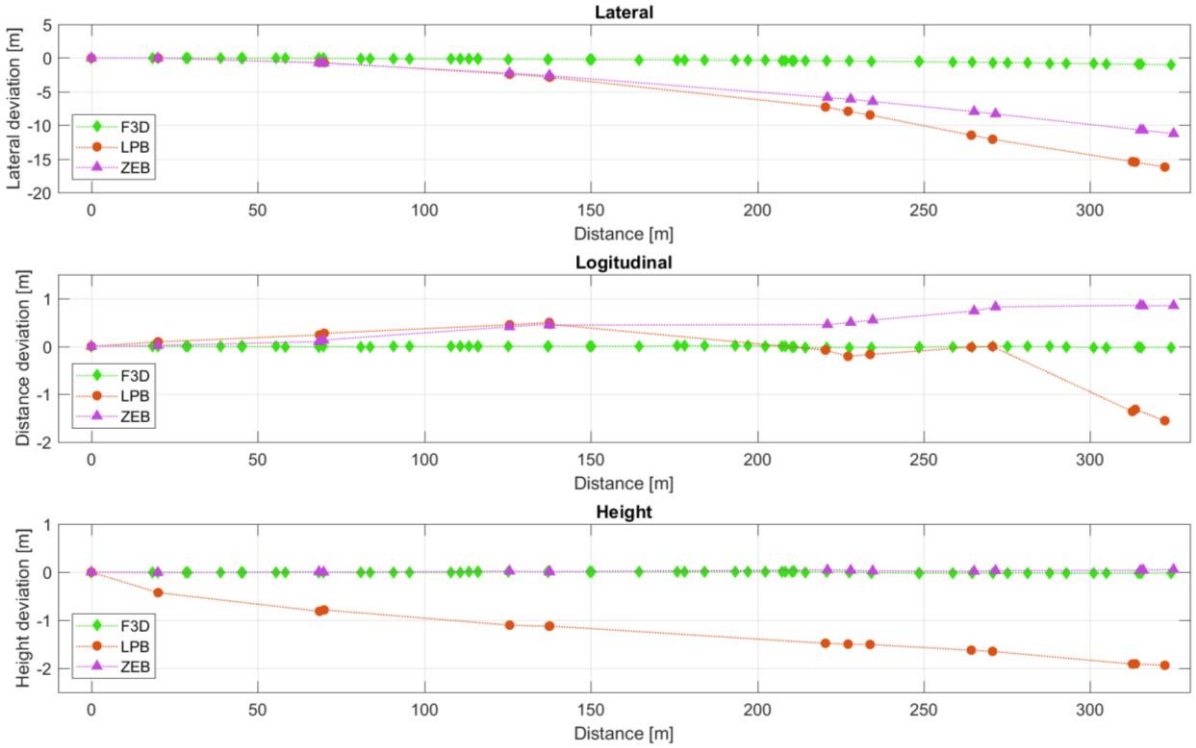

Figure 3: Lateral, longitudinal and height displacements between the point clouds and points of the terrestrial network. Note the different scale for the lateral deviation

To check, to which degree the linear part of the observed coordinate drift, and the scale may be due to inaccuracies of the sphere centres as detected within the point clouds the displacements at the end of the mine are downscaled to the 20 m baseline length. The results are given in Table 3. The lateral displacements of 0.06 m (F3D), 1.00 m (LPB) and 0.69 m (ZEB) over 20 m are on the order of one sphere radius for F3D and ten sphere radii for LPB and ZEB. This is far more than what could be explained by potential inaccuracies of the sphere centre detection within the point clouds, e.g. due to noise and limited point density. Thus, the deviations at the end of the mine are a result of uncompensated drift rather than inaccurate georeferencing. This indicates that ground control (or reference) points or other means of stabilizing the point clouds are needed to obtain higher absolute accuracy.

Scale deviations and overall rotations can be addressed by applying a similarity transformation using reference points at both ends of the mine. The results obtained after carrying out such a transformation using three GCPs near the entrance and three near the end of the mine are also shown in Table 3. The values represent the deviations from further reference points (not used for the transformation) in the middle of the mine. They indicate that even after this rigid transformation significant deviations still exist, especially for the lateral component of the LPB (-3.82 m) and ZEB (-1.93 m) point cloud.

This analysis shows that the non-linear drift needs to be compensated for all measurement systems used herein if cm-level accuracies are needed throughout the mine.

Table 3: Displacements (lateral, longitudinal and in height) of the point clouds with respect to the TPS network (all values are given in metres)

	a) At the end of the mine, georeferenced using 2 GCPs near entrance			b) Values from a) downscaled to the 20 m baseline between the 2 GCPs			c) At the center of the mine after georeferencing using 3 GCPs at the entrance and 3 at the end		
	Lat.	**Long.**	**Height**	**Lat.**	**Long.**	**Height**	**Lat.**	**Long.**	**Height**
F3D	1.02	-0.03	-0.02	0.06	0.00	-0.00	-0.20	-0.01	-0.01
LPB	16.21	-2.00	-1.94	1.00	-0.12	-0.12	-3.82	-0.94	0.19
ZEB	11.24	0.63	0.05	0.69	0.04	0.00	-1.93	-0.04	0.11

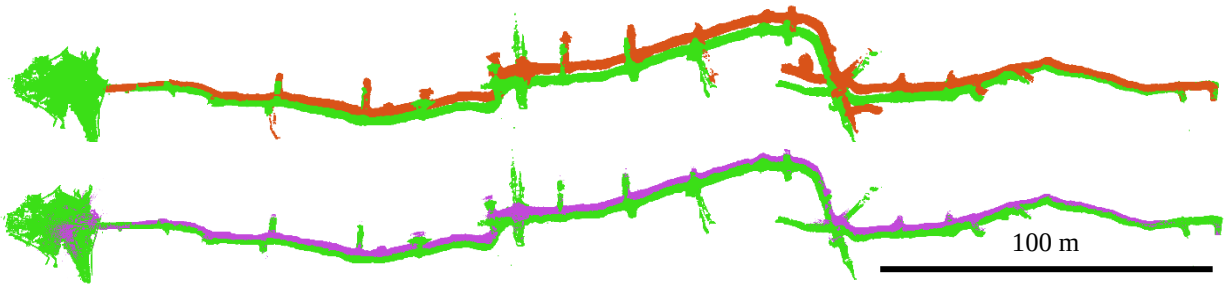

Figure 4: Differences between point clouds after rigid transformation using 3 GCP near the entry and 3 GCP near the far end of the mine (version c) as of Table 3): F3D (green), LPB (red) and ZEB (violet).

3.3 Non-rigid transformation

Deformations of a point cloud – as resulting from sensor drift or accumulated registration deviations in this study case – cannot be mitigated using a rigid-body or similarity transformation. If the respective system allows using GCPs directly within the raw data processing, this may mitigate the remaining deviations. If the system is or is operated as a black box outputting registered/georeferenced point clouds like the MM in our study case, a different approach is needed for drift mitigation. We propose to use non-rigid transformation based on a sufficient number of GCPs distributed throughout the mine. Each of these GCPs needs to be identified within the point cloud. The resulting displacement vectors between point cloud and given GCP coordinates can then be spatially interpolated to obtain displacement vectors for all points within the point cloud. Shifting each point by the corresponding displacement vector then corresponds to a non-rigid transformation, which can reduce the deformations of the point cloud. Typically, for preserving the high relative accuracy of neighbouring parts of the point cloud, the chosen interpolation must assure that a closer GCP has a larger influence on the transformation vector of a single point than a GCP at farther distance.

Unfortunately, no standard software for such non-rigid transformations was known or available to the authors. Three established spatial interpolation schemes, namely nearest-neighbour, triangle based interpolation and distance weighted interpolation, were therefore applied using a proprietary implementation in Matlab. We found out that the nearest-neighbour interpolation results in undesired discontinuities, and the triangle based approach fails in the present case because of the geometric configuration: the GCPs are located almost along a line and very long, narrow triangles result from the triangulation. However, the distance weighted interpolation yielded a clear improvement in this specific case. Using all 16 GCPs marked by spheres during the MM data acquisition the displacement vectors $\boldsymbol{v}_i$ at the sphere centres were computed. For each point of the cloud a displacement vector $\boldsymbol{v}(\boldsymbol{X})$ was then calculated as a weighted sum of the $\boldsymbol{v}_i$vectors at the GCPs according to

$$\boldsymbol{v}(\boldsymbol{X}) = \sum_{i=1}^{16} \frac{\boldsymbol{v}_i}{\|\boldsymbol{X} - \boldsymbol{X}_i\|^2} \tag{1}$$

where the inverse of the squared distance between the interpolation point $\boldsymbol{X}$ of the point cloud and the respective GCP $\boldsymbol{X_i}$ is used as weight. The squared distance in the weight factor was chosen empirically as it produced the best result in this study case. The results obtained starting from the LPB point cloud are shown in Figure 5 which displays the differences between the F3D point cloud and the non-rigidly transformed LPB point cloud. The results obtained using this simple non-rigid transformation are apparently already much better than those obtained without taking the GCPs into account and help to bring the accuracy of the LPB results to about the level expected if loop closures were available and the actual distances remained above the minimum distances of the sensors.

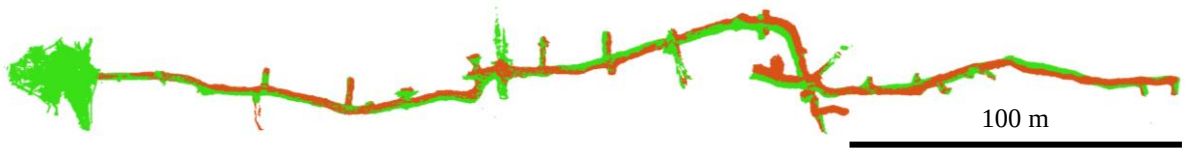

Figure 5: Non-rigidly transformed LPB data (red) using the F3D sphere centres as GCP (green)

The results shown above indicate that it is worth considering non-rigid transformations for improving underground MM point cloud accuracy. However, further investigations are needed to (i) provide guidelines for the number and location of required GCPs for further reduction of the deviations, and (ii) for selection of the most appropriate spatial interpolation function. It is to be expected that the two questions are linked and need to be investigated jointly. These investigations are left for future work.

4. VISUALIZATION

Visualization of geodetic data can be extremely useful when developing a project in collaboration with people with or without any specific technical background, where it is necessary to extract information out of the acquired data. Additionally, the project may have a nontechnical purpose where data representation is of main interest. For this project, several different innovative approaches of visualizing the acquired data were carried out, namely a video animation, a 3D model print, and a virtual reality visualization. In addition, an interactive website is used for publishing the project results and making them accessible to a wider audience.

A mesh has to be generated out of the point cloud, as the first step for all the different visualization approaches. The appropriate settings were chosen empirically, considering the high point density of the original dataset, the desired resolution of the mesh and its visual appearance, file size, etc. The imported raw point cloud has to be cleaned from artefacts and later down-sampled. For the F3D data and the ZEB data, we have used a subsampling radius of 1.5 cm, in order to substantially reduce the number of points within the dataset and bring the resolution to approximately the same level as the one that had been chosen by Leica for the LPB data processing. Afterwards point normals were computed using quadratic local surface models, which are suitable for local approximation of curvy and complex surfaces. We chose to determine the orientation of the normals from samples of 40 points, respectively. After the point clouds had been prepared in that way, the mesh was generated using the triangular mesh generation algorithm (Poisson surface reconstruction). All these steps for the preparation of the point clouds for visualization have been carried out using CloudCompare.

4.1 3D model print

The mesh of the gold mine represents the surface separating void space from solid rock/surrounding material. For 3D printing, it has to be placed within a frame that supports the whole structure (e.g. a box casing). To give the user access to the interior of the mine in this 3d print, the box has to open up. We decided to realize this by splitting the entire model into an upper and a lower part and allow the two parts to be folded together. The model for 3d printing was therefore created using Boolean operations (e.g. subtraction) between two initial elements – the mesh of the mine and the created box element. The walls of the created model have no thickness, therefore a certain thickness needs to be added, depending on the printer specifications, settings, and the used material (gypsum print requires a minimum thickness of 2 mm). We have additionally labelled the physical model by adding 3D text to the model. Figure 6 shows the printed parts of the model. The preparation of the data, starting from the generated mesh takes a couple of hours, primarily depending on the file size of the mesh and the performance of the used computer. Additionally, the duration of the 3D print depends on the printer specification, settings (e.g. detail resolution) and the chosen material.

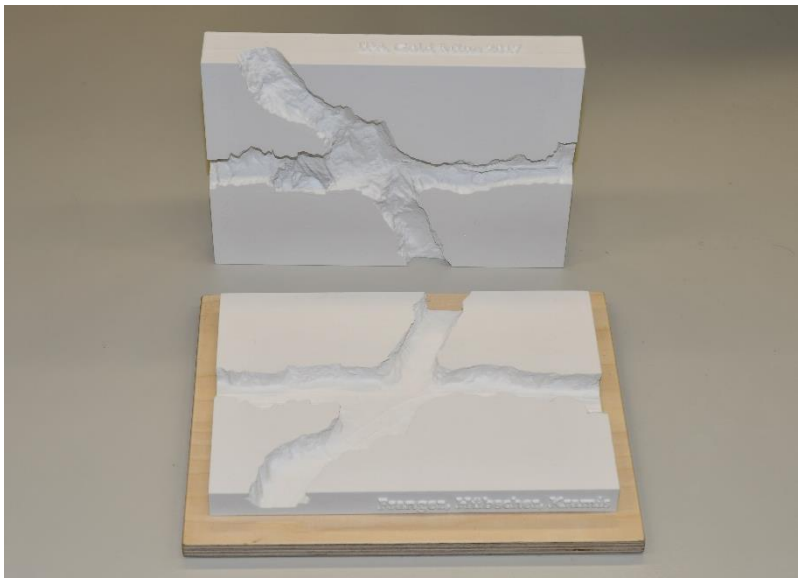

Figure 6: A picture of the printed 3D model of a cross intersection.

4.2 Video animation

A fly through animation of the point cloud data was created using the Bentley Pointools V8i. Within the software, it is required to specify the poses and further parameters of the camera along its desired path through the model. The effort and difficulty of creating the video animation is low, however the time required to render the animation can take a few hours, depending on the specified output settings (resolution, codec, video length, frames per second, etc.). The final video obtained using the LPB point cloud, which was the only one in this study containing RGB information, and thus the most suitable one for this type of visualization has been published on YouTube[8].

4.3 Virtual reality

We have also visualized the mesh in a virtual reality (VR) environment using the HTC Vive headset. The visualization is achieved using the Unity game engine. We have designed three levels of information (Figure 7) between which the viewer can freely change. The levels differ in terms of information content and type of display.

The mesh representing the third level (c) was obtained by down-sampling the F3D point cloud, since Unity does not perform well when using large data files (above 700 MB). Besides the mesh, a point cloud is visualized and imported in Unity using the asset package Point Cloud Viewer and Tools available on the Asset Store. The visualization of the model of the galleries

[8] Gold Mine Visualization using Leica Pegasus:Backpack Data: https://www.youtube.com/watch?v=8VGN8Ccf2Rc&t

was fused with a digital terrain model (DTM), topographic and geological maps (together with a legend of displayed rocks and minerals), as shown on the first (a) and second (b) level in Figure 7. The DTM of Switzerland was obtained from swisstopo[9] and the data extending over the border to northern Italy were acquired from the European Environment Agency[10] offering open source data.

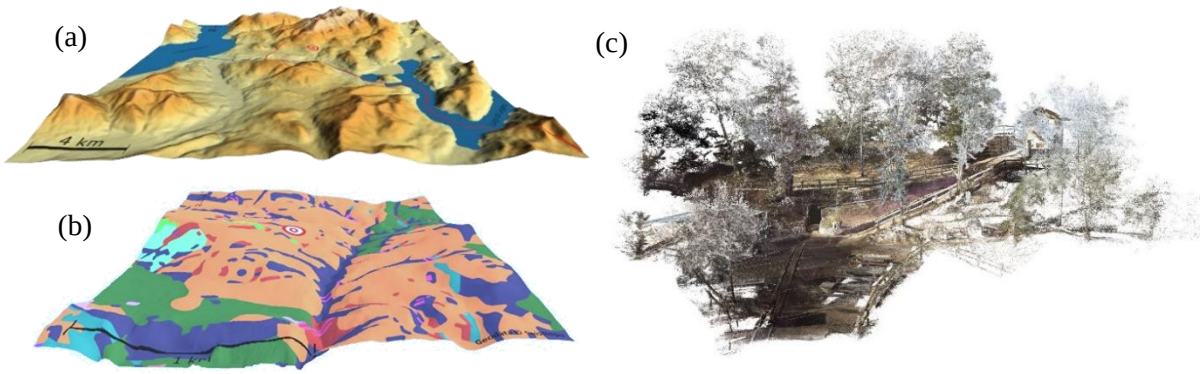

Figure 7: (a) First level of visualization using a topograpic map and a DTM; (b) second level of visualization using a geological map and a DTM; (c) third level of visualization using a point cloud and a mesh

4.4 Online platform

Additionally, an interactive website is created for publishing the project results to the wider audience using three individual approaches. The website is built up on Bootstrap, an open source toolkit for developing with HTML, Cascading Style Sheets (CSS) and JavaScript.

The mesh generated from the F3D point cloud has been uploaded using Sketchfab. The platform has a size limitation on the uploaded data of 50 MB. Therefore, the original point cloud was down-sampled from 300 million to approximately 2 million points. This took around one hour on a standard PC. Due to down-sampling the level of detail is of course reduced considerably, but this is not a problem since the goal of the publication on the website is to convey an impression about the mine, not to provide data for a technical analysis.

We have used Potree to visualize the coloured point cloud acquired by LPB. This is a web-based renderer for large point clouds developed by Schütz (2016). The displayed point cloud contains approximately 26 million points. Potree uses a hierarchical data structure with data stored in sets of different resolutions. Because of this structure the whole point cloud can be streamed and rendered within seconds. To create the corresponding rendered model took less than halfe an hour on the PC mentioned above.

[9] https://shop.swisstopo.admin.ch/en/products/height_models/dhm25
[10] https://www.eea.europa.eu/data-and-maps/data/eu-dem

The data captured by the ZEB was visualized using Blend4Web Community Edition. This is an open source platform allowing to publish computer graphics online. The point cloud data need to be considerably down-sampled (in our case from approx. 6.5 million points to 800'000 points). On the other hand, the website then loads within a few seconds. The data are prepared in the open source software Blender to obtain the desired appearance (surface colour, reflectance, shadowing, etc.) and then exported into an HTML file ready for the upload[11]. To prepare a scene using this approach still requires significant manual interaction and took about a day in our case.

Sketchfab has the advantage that a mesh can be uploaded directly on the platform website, no additional server is needed. This makes the handling easy and needs little time. The size limitation on the uploaded data is a major restriction of this platform. Potree is the only platform where the full point cloud can be uploaded without the need to down-sample the data. However, no mesh visualization is possible. Blend4Web offers many adjustments to create the desired appearance of the scene. Preparation is more time consuming for this software compared to the other two platforms, and the mesh must be down-sampled significantly, because the browser can otherwise not load the HTML file.

5. COMPARISON OF THE APPROACHES

5.1 Data quality and information content

The accuracy of the registered point clouds in terms of overall accuracy has been described above (sec. 3). Using subsets of the data (indicated in
Figure *8*) more specific aspects are briefly assessed in this subsection.

Figure 8: Locations of subsets used for detailed analysis

The spheres located within the mine play a crucial role in this paper, as they are used (i) to establish a common coordinate system for all point clouds, and (ii) to assess the quality of the registered point clouds. One of these spheres is shown in Figure 9 as represented within different point clouds. They differ in amount, distribution and accuracy of the points due to the different acquisition techniques, measurement processes and settings during both acquisition and processing. The sphere is readily recognizable in the point cloud of the F3D because of the high number of points (1828 pts) and low noise, largely due to the short distance between scanner and sphere. The data provided by the LPB are comparatively sparse because they had

[11] The website is available at: https://digitalreality.ethz.ch/goldmine

been reduced to a nearly constant point spacing of 2.5 cm for the entire mine by the Leica operator. This yields a point cloud appropriately balancing detail versus file size for the entire mine, but results in apparently few points (192) on the small spheres. While this impairs the visual impression when just looking at the point clouds, and made the manual separation between potential sphere points and other points (e.g. surrounding walls) harder, the number is still sufficient to estimate the center of the sphere accurately for the analyses mentioned within this paper. The ZEB data (2909 pts) show a very noisy, apparently egg-shaped point cloud instead of a sphere. The shape is most likely the result of merging the data of forward and backward acquisition fully automatically carried out by the respective software. The point density at the sphere is apparently much higher than with the LPB although the full point clouds of the mine have almost the same amount of data (see Table 2). The reason is that the ZEB operator intentionally slowed down while walking past the spheres, moved closer and tried to acquire the spheres with particularly many points, while the operation of the LPB required maintaining nearly uniform walking speed and no special precautions were taken for dense acquisition of the spheres.

Figure 9: Comparison of a sphere (radius 75 mm) as found in the point clouds avaialble for analysis (from left to right: F3D, LPB, ZEB)

The point clouds obtained from the different techniques show very different distribution of point densities over the whole mine (see Figure 10). As a stationary instrument with fixed angular resolution, the F3D yields point densities decreasing linearly with distance. In the present case, the highest density (~100'000 pts/m^2) is found just above the instrument's position while the lowest density (~20'000 pts/m^2) is found between the instruments and on the floor. Due to the voxel-based filtering during processing, the LPB yields a point cloud with almost constant point density (~6'000 pts/m^2) except along two longitudinal sections of the ceiling (~12'000 pts/m^2). ZEB shows an irregular pattern of point density ranging from about 3'000 pts/m^2 to about 20'000 pts/m^2; this reflects the non-uniform movement of the observer and the varying distances.

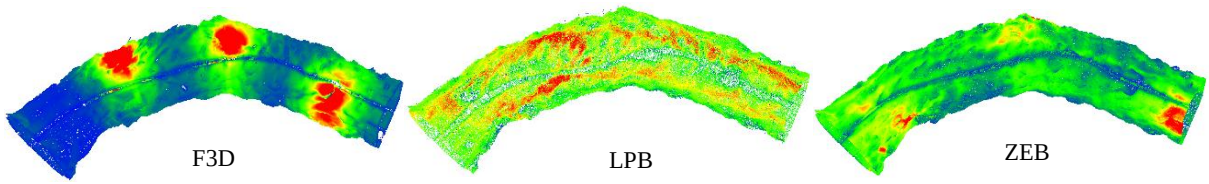

Figure 10: Point cloud density (different color map for the three images because of vastly different point densities; red: high density, blue: low density).

Cross-sections of the point clouds (see Figure 11) highlight the different noise levels, which are mostly due to the different sensors involved and correspond to the respective specifications. The static scanner (F3D) shows accordingly the highest precision. The LPB yields point clouds with unevenly distributed noise exhibiting a much higher noise level in the upper half of the cross-sections throughout the mine. We attribute this to the fact that the distance between the sensors and the corresponding surfaces was less than 0.5 m and thus below the minimum working range as specified by Leica. This suggests that data acquisition may be possible even outside the specified range but at the cost of reduced precision. ZEB shows almost constant noise level throughout the mine, but the point clouds are slightly noisier at areas which were scanned with higher point density, e.g. close to the spheres.

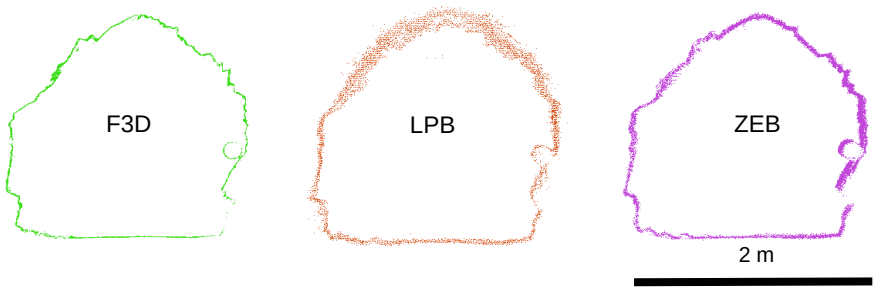

Figure 11: Cross-sections of 5 cm width showing the noise levels of the point clouds and their spatial distribution at the identical location within the mine.

Based on the specifications and the results of the above accuracy analysis, the F3D point cloud seems to be the geometrically most accurate one. We have analysed deviations of the MM results from this one also on a more local scale than above. A mesh-to-mesh (M2M) comparison of an 8 m long section is shown in (Figure 12). The ZEB data mostly show small apparently random deviations between -1 cm and 1 cm throughout the whole area, which is well within the specification. The LPB results show systematic deviations exceeding 5 cm, again primarily in the upper part of the gallery and probably linked to the operation outside the specified working range. The M2M analysis was performed in GOM Inspect, while for all the other analyses presented in this section CloudCompare was used.

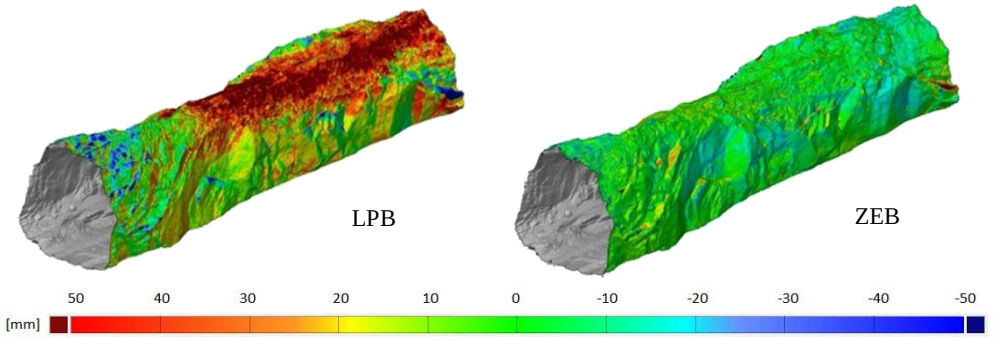

Figure 12: M2M comparison with F3D mesh as reference

While the LPB acquires RGB values for each point inherently, the F3D dataset shows only reflectivity information in addition to the coordinates of the points. The ZEB provides neither RGB nor reflectivity information. RGB information could have been acquired with the F3D at the expense of approximately 50% increased scanning time. However, this would only have worked appropriately if the galleries had been floodlighted sufficiently.

5.2 Technique comparison

The criteria to compare the deployed techniques and their results include the time of scanning and processing, instrument handling, data complexity and accuracy, acquisition of additional information (e.g. colour), etc. All the used instruments can be operated by a single person who completed a system handling training. The LPB requires a basic training of 5-7 days for data capture, processing and feature extraction, according to the manufacturer. The ZEB can be used after an introduction of about an hour and by following the provided system manual, and the training required for using the F3D and pre-processing its data to obtain a filtered and registered point cloud is in the order of 1-2 days.

The F3D produced the best results in terms of bending, scale and lateral drift of the point clouds as compared to the terrestrial network. The multiple acquisition settings allow using the instrument according to the available time frame and required data quality. The major downside of its use is the extended acquisition time. The resulting files are very large with vastly different point densities depending on scanner-to-surface distances. Handling of the data is complex and time-consuming if manual interaction is required (like for clicking onto the spheres and starting manual registration in our case). Due to the rough surfaces, it might have been possible to do it without spheres and register the point clouds directly using the iterative closest point (ICP) algorithm (Besl and McKay (1992), Chen and Medioni (1991)). However, we would have needed more overlap of the point clouds in that case and thus more scans. In our case spheres at selected locations were used anyway for some of the analyses within this paper.

The advantage of LPB is the fast acquisition process, its mobility as compared to the F3D, and the fact that useful RGB data are acquired along with the geometric data and without extra time or effort. The instruments mobility, achieved by the backpack assembly, on the other hand represents a limiting factor in very narrow spaces with low-ceiling like in this case due to the backpack's height when being worn. Actually, as stated above, the system had to operate below its minimum specified distance within this mine. Targets or spheres placed in the scene are not required. The generation of the final point cloud out of the raw data required approximately four times the acquisition time length. A disadvantage in comparison with TLS is the lower precision and the increased challenge to mitigate drift in case of unavailability of GNSS data.

The ZEB system, including the data processing part, has the advantage of being easy to use. In particular, compared to F3D the acquisition time is very short. Because the scanner is handheld, the user can move more freely than with a backpack system (like e.g. LPB). This was a clear

advantage in this narrow mine allowing also to increase point density at locations where this was deemed useful (e.g. around spheres). The export and point cloud generation are fast and require low effort. Targets or spheres placed in the scene are not required and the final point cloud is generated automatically. Since no colour or intensity information is obtained, the data are not as suitable for visualization purposes as the other data. There are very little opportunities for the user to custom tailor parameters of data acquisition or data processing if needed.

6. CONCLUSIONS

The paper provides a comparison between three innovative technologies for 3D data acquisition. Besides discussing the major advantages and disadvantages of the used instruments, an empirical comparison is done. The comparison is based on various criteria: time consumption, complexity of data processing, point cloud accuracy, etc. Since only one dataset was acquired for each instrument, all the results are indicative only. A thorough accuracy analysis based on a statistically valid sample would be highly interesting but is beyond the scope of this paper. The paper involves new technological alternatives (LPB and ZEB) to well-established terrestrial laser scanning (F3D) that are nowadays available on the market. Even though the MM solutions have certain disadvantages, their use starts to address a wide range of new application cases, which can also be of interest outside the surveying community. Additionally, visualization of the geodetic data is becoming more and more important when being used for touristic, architectural, archaeological, etc. purposes and therefore need to be attractively presented. Several innovative approaches for visualizing the laser scanning data are presented in the paper, making use of emerging technologies such as 3D print and VR.

The discussion of the results of the project illustrates the technical and practical advantages and disadvantages of each technique. The pros and cons are summarized in Table 4, allowing the user to identify whether the instrument will produce the most optimal results within certain application.

Table 4: Summary of pros and cons of the techniques

	F3D	LPB	ZEB
Pros	- Overall the best performance when recording complex surfaces over larger scale, in terms of data quality (low effects of bending, scale and lateral drift), - acquisition when high data accuracy and resolution are of importance, - optional acquisition of RGB and intensity information.	- Very fast acquisition without much effort, - targets/spheres not necessary in the scene when scanning, - acquisition when precision of a few cm is required and the absolute accuracy is of minor importance, - optional acquisition of RGB information (allows further visualization purposes).	- Very fast acquisition and preprocessing of the data (point cloud creation) and without much effort, - acquisition when precision of a few cm is required and the absolute accuracy is of minor importance, - handheld therefore more flexible acquisition possible.

Cons	- High time consumption for scanning (10 times longer as compared to the other techniques), - targets/spheres necessary in the scene when scanning, - high data complexity and its handling (e.g. manual registration).	- Lower specified precision and lower accuracy due to more prominent drift, - backpack's height when worn makes it hard to scan narrow and low-ceiling environments, - preprocessing of the data (point cloud generation) is not straight forward and long software training is required.	- Lower specified precision and lower accuracy due to more prominent drift, - little opportunity to custom tailor parameters of data acquisition, - it does not provide RGB or intensity information, therefore the data cannot be used for certain visualization purposes.

ACKNOWLEDGMENTS

We would like to thank everyone who was involved and helped to execute the project throughout the semester. Especially Leica for providing the backpack, carrying out the data acquisition and providing the processed data for free and Allnav for providing the ZEB-REVO. E. Serantoni, Z. Gojcic (ETH) provided support throughout the project, the association "Miniera d'oro di Sessa" (A. Passera, G. Zanetti) assured support during data acquisition, A. Wieser (ETH) gave feedback on an earlier version of the paper, and geosuisse awarded a grant enabling participation at the conference.

REFERENCES

Besl P, McKay N (1992) A Method for Registration of 3-D Shapes. IEEE Trans. Pattern Anal. Mach. Intell. 14:239–256.

Chen Y, Medioni G (1991) Object modeling by registration of multiple range images. Proceedings 1991 IEEE Int Conf Robot Autom 2724–2729.

Farella, E. M. (2016). 3D Mapping of Underground Environments With a Hand-Held Laser Scanner. In Proc.: 61° Convegno Nazionale SIFET, June 8-10, Lecce.

Schütz, M. (2016). Potree: Rendering Large Point Clouds in Web Browsers. Diploma thesis, Vienna Institute of Computer Graphics and Algorithms, Vienna University of Technology.

Sirmacek, B. et al. (2016). Comparison of ZEB1 and Leica C10 Indoor Laser Scanning Point Clouds. ISPRS Annals of the Photogrammetry, Remote Sensing and Spatial Information Sciences, Volume III-1, pp. 143-149

Umeyama, S. (1991). Least-Squares Estimation of Transformation Parameters Between Two Point Patterns. *IEEE Transactions on Pattern Analysis and Machine Intelligence*, vol. 13, no. 4, pp. 376-380.

Wieser, A., Lienhart, W. and Brunner, F.K. (2003). Nachbarschaftstreue Transformation zur Berücksichtigung von Spannungen im amtlichen Festpunktfeld. VGI – Österreichische Zeitschrift für Vermessung und Geoinformation, vol. 91 (2), pp. 115-121.

Zlot, R. and Bosse, M. (2014). Efficient Large-Scale 3D Mobile Mapping and Surface Reconstruction of an Underground Mine. In: Yoshida K., Tadokoro S. (eds) Field and Service Robotics. Springer Tracts in Advanced Robotics, vol 92. Springer, Berlin, Heidelberg, pp. 479-493.

BIOGRAPHICAL NOTES

Valens Frangez, Benjamin Kramis and Florian Hübscher are MSc students in Geomatic Engineering at ETH Zürich. Andreas Baumann is a junior researcher at the Institute of Geodesy and Photogrammetry, ETH Zürich.

CONTACTS

Andreas Baumann
Institute of Geodesy and Photogrammetry
ETH Zürich
Stefano-Franscini-Platz 5
8093 Zürich, Switzerland
Email: andreas.baumann@geod.baug.ethz.ch